KONSTAN
JURNAL FISIKA DAN PENDIDIKAN FISIKA
Volume 10, Number 2, December 2025
E-ISSN : 2460-9129 dan P-ISSN : 2460-9110
http://jurnalkonstan.ac.id/index.php/jurnal

Optical Band Gap and Urbach Energy of Cobalt-Doped Magnetite Nanoparticles Derived from Loang Balok Iron Sand

Kormil Saputra[1], Rahmatun Inayah[2], Ika Umratul Asni Aminy[3], Teguh Ardianto[4], Dian W. Kurniawidi [5,*)]

[1,2,3,4,5)]*Physics Study Program, Faculty of Mathematics and Natural Sciences, University of Mataram, Indonesia*

* E-mail correspondence: diankurnia@unram.ac.id

Article Info:

Sent:
August 22, 2025

Revision:
December 03, 2025

Accepted:
December 9, 2025

Keywords:

Cobalt-doped magnetite, Natural Iron Sand, Tauc plot, Kubelka-Munk, Urbach energy

Abstract

Doping is a practical approach to altering a material's electronic and structural properties, thereby influencing its optical and magnetic characteristics. This study successfully synthesized and characterized cobalt-doped magnetite (Fe2.5Co0.5O4) nanoparticles from natural iron sand via coprecipitation. The main objective was to evaluate the optical properties of the synthesized material using UV-Vis spectroscopy and to compare band gap energies using three approaches: the Tauc method (direct and indirect transitions), the Kubelka–Munk method, and the Urbach energy, an indicator of structural disorder. The characterization results revealed that the incorporation of Co2+ ions into the magnetite structure induced significant changes in the absorption spectra, including the emergence of new peaks and a redshift in the wavelength. The obtained band gap values were 3.71 eV (Tauc-direct), 2.18 eV (Tauc-indirect), and 2.33 eV (Kubelka–Munk), confirming the presence of two types of optical transitions. Furthermore, the relatively low Urbach energy (0.07138 eV) indicated that the crystal structure remained well-preserved despite the modifications induced by doping. This study highlights the importance of employing multi-method approaches for reliable optical characterization and demonstrates that Fe2.5Co0.5O4 materials derived from local resources possess promising potential for photocatalytic and optoelectronic applications.

INTRODUCTION

In the modern era marked by the revolution in material technology, the search for functional nanostructured materials has become increasingly important to meet the demands of various strategic applications, ranging from renewable energy to information technology and biomedicine [1]. Among the most prominent classes of materials are semiconductors with tunable magnetic and optical properties. Such materials are highly sought after for use in photonic devices, optical sensors, battery electrodes, and spintronic-based energy storage systems [2]. Within this category, spinel ferrites with the general formula MFe2O4 (M = divalent metals such as Co^{2+}, Zn^{2+}, Ni^{2+}, and others) stand out due to their high stability, strong magnetic properties, and flexible crystal structures [3], [4], [5]. Magnetite (Fe_3O_4), as one of the ferrite members, is the most extensively studied ferrimagnetic material because of its good conductivity, high chemical stability, and tunability through cationic substitution [4]. However, to enhance performance and expand its potential applications, various modification strategies have been pursued, including doping.

Doping is a practical approach to altering a material's electronic and structural properties, thereby influencing its optical and magnetic characteristics [5]. In the case of magnetite, partial substitution of Fe ions with Co ions yields cobalt-doped magnetite ($Fe_{3-x}Co_xO_4$), which exhibits

significant improvements in magnetic field strength, light absorption, and structural stability [6]. These changes are particularly crucial for the design of innovative materials for applications such as photocatalysis, data storage, and magnetic-field-based biosensors. One of the most critical aspects of evaluating the performance of semiconductor materials is analyzing the band gap energy, which is the minimum energy required to excite an electron from the valence band to the conduction band.

The band gap determines a material's optical response, specifically the range of wavelengths it can absorb or transmit. Modifying the band gap through doping can shift the optical response, making the material more effective at harvesting visible or ultraviolet light. Cobalt has been shown to either reduce or increase the band gap depending on the local structure and synthesis conditions [7]. Moreover, the presence of structural defects or crystalline disorder induced by doping can be analyzed through the Urbach energy. Urbach energy is a parameter that reflects the degree of disorder in the crystal lattice, leading to the formation of tail states in the energy band. A higher Urbach energy indicates greater disorder, which negatively affects charge-carrier mobility and optical transition efficiency [8]. Therefore, Urbach energy analysis provides important additional insights into the crystalline quality of the synthesized materials.

In efforts to support sustainability and self-reliance in raw materials, approaches that leverage local resource potential have become increasingly relevant. Indonesia possesses substantial iron mineral resources comprising approximately 17% primary iron ore, 8% iron sand, and 75% lateritic iron ore, yet iron sand is still predominantly exploited as a low-value raw material [4]. Recent reports estimate national iron ore reserves of around 2.9 billion tons (about 1.7% of global reserves), with annual iron sand production on the order of 16.6 million tons. At the same time, a significant fraction of this material is exported or used in basic industries such as cement rather than being upgraded into high-value functional materials. This situation contrasts with the growing demand for magnetic oxides, microwave absorbers, and photocatalysts in energy, environmental, and electronic applications, which are often imported or synthesized from high-purity commercial precursors. Several studies have highlighted that Indonesian iron sand, when combined with appropriate processing technologies, can be transformed into advanced materials such as $TiO_2/Fe2O_3$ photocatalysts [9], magnetic nanocomposites [10], and microwave-absorbing fillers [11], demonstrating its potential as a strategic raw material for value-added products in the domestic materials industry. Consequently, developing synthesis routes that directly convert local iron sand into functional cobalt-doped magnetite and systematically assessing their band-gap characteristics is an important step toward linking national mineral resources with targeted optoelectronic and photocatalytic applications.

On the regional scale, the coastal sand of Mataram City, including Gading, Loang Baloq, Penghulu Agung, and Ampenan beaches, is known to be rich in iron-bearing minerals [12]. Systematic characterization of these sites showed that the magnetic mineral fraction in Loang Baloq beach sand reaches about 93.5% of the bulk sand mass, indicating a very high content of magnetically active phases. Atomic absorption spectroscopy and XRF measurements further revealed that the magnetic sand from these beaches contains Fe in the range of 10.6–16.3 mg/g, with Loang Baloq exhibiting an Fe elemental content of about 62.1 wt% and an oxide composition dominated by Fe_2O_3 (51.5 wt%), SiO_2 (24.3 wt%), and TiO_2 (6.6 wt%), accompanied by smaller amounts of CaO (3.3 wt%), Al_2O_3 (8.3 wt%), and minor MnO, MgO, and other trace oxides [12]. XRD analysis confirms that the main magnetic phases present at Loang Baloq are magnetite and hematite (α-Fe_2O_3), consistent with reports on Lombok and other Indonesian iron sands where magnetite, hematite, maghemite, and ilmenite are identified as dominant or significant constituents.

The synthesis of cobalt-doped magnetite based on local iron sand resources is also in line with global trends in green and renewable resource-based material development. Previous studies have reported that the use of natural sources does not compromise the quality of the synthesized products, and in some cases, the presence of natural impurities may even enhance material properties [10], [13], [14]. Furthermore, the co-precipitation method, widely adopted in many studies, offers advantages such as procedural simplicity, low cost, and effective control over particle size [15]. In semiconducting and semimetallic oxides, the optical band gap is a central parameter because it determines the spectral range of light absorption, carrier excitation processes, and ultimately the suitability of a material for

photocatalytic and optoelectronic applications [2]. For spinel ferrites with general formula MFe_2O_4 (M = Fe, Co, Ni), the band gap is governed by the crystal field around the metal cations and the Fe–O–Fe (or M–O–Fe) superexchange paths, so that cation substitution offers a direct route to tune their electronic and magnetic behaviour. When Co^{2+} ions partially replace Fe cations in magnetite, the Co 3d levels modify the electronic structure and can narrow the band gap and shift the absorption edge toward the visible region. Todou Assaouka et al. [16] showed that increasing cobalt concentration in magnetite nanoparticles reduces the band gap from about 2.1 eV to 1.8 eV, implying enhanced optical activity under visible light, while Lachowicz et al. [17] reported dual band gap behaviour in cobalt ferrite that they attributed to crystalline domains with different degrees of structural order. Such observations indicate that cobalt doping may simultaneously change the magnitude of the band gap, generate more than one type of optical transition (direct and indirect), and introduce disorder-related tail states near the band edges. From an optoelectronic perspective, direct band gap transitions are associated with strong optical absorption and efficient photogeneration of carriers in thin layers, whereas indirect transitions, which are phonon-assisted, can influence carrier lifetime, transport, and recombination dynamics; the balance between these two types of transitions is therefore critical for optimizing photocatalysts, photodetectors, and other light-driven devices based on ferrite nanoparticles [18], [19].

In this context, cobalt-doped magnetite derived from iron sand is a promising candidate for visible-light photocatalysis, magnetic photocatalysts that can be easily separated from reaction media, magneto-optical sensors, and functional components in energy-related devices such as photoelectrodes or absorber layers. A detailed, quantitative determination of the optical band gap considering both direct and indirect Tauc analyses together with Kubelka–Munk treatment of diffuse reflectance and evaluation of the Urbach energy as a measure of band-edge disorder is therefore essential to link the electronic structure of $Fe_{2.5}Co_{0.5}O_4$ to its potential performance in photocatalytic and optoelectronic applications. Nevertheless, few studies have systematically verified changes in band gap values by directly comparing these three computational approaches within the context of nanoparticles synthesized from natural resources. This becomes particularly important as each method operates under different assumptions regarding the type of transition and the interaction of light with the material. The present study aims to address this gap by synthesizing $Fe_{2.5}Co_{0.5}O_4$ nanoparticles from natural iron sand and comparing band-gap calculations obtained using the Tauc (direct and indirect) and Kubelka–Munk methods, along with Urbach energy analysis as an indicator of structural disorder.

The overall objective is to investigate the optical characteristics of cobalt-doped magnetite nanoparticles synthesized from natural iron sand, particularly using UV-Vis spectroscopy to determine the band gap and Urbach energy. By adopting a holistic, resource-based approach, this study seeks to broaden understanding of low-cost, environmentally friendly ferrite-based semiconductor materials with strong potential for future technological applications.

METHOD

Synthesis and Characterization of $Fe_{2.5}Co_{0.5}O_4$ Nanoparticles Using Coprecipitation Method

The natural iron sand used in this work was sourced from Loang Balok Beach (Mataram, Indonesia) and corresponds to the same material previously characterized by Susilawati et al. [12]. Prior to dissolution, the sand was washed several times with distilled water to remove adhering salts and organic debris, dried at 105°C overnight, and then annealed in air at 400 °C for 3 h to reduce volatile impurities and stabilize the iron oxide phases. The target composition followed the general spinel formula $Fe_{3-x}Co_xO_4$ with x = 0.5, corresponding to a Co^{2+}:Fe (Fe^{2+}/Fe^{3+}) molar ratio of 0.5:2.5. To prepare the precursor solution, 20 g of the pre-treated iron sand were dissolved in 58 mL of 38% HCl (Merck, India) under magnetic stirring at room temperature for 2 h to extract Fe^{2+}/Fe^{3+} ions. The slurry was then filtered to remove undissolved residues, yielding a clear $FeCl_2/FeCl_3$ solution. In a separate beaker, 5.06 g of $CoCl_2 \cdot 6H_2O$ (Merck, India) (0.0212 mol Co^{2+}) were dissolved in distilled water and subsequently mixed with the Fe-containing solution under vigorous stirring at 600 rpm. Based on the stoichiometric calculation, the Fe solution obtained from the iron sand provided

approximately 0.106 mol of total Fe ions, so that the overall Co:Fe molar ratio in the mixed solution was close to 1:5, which corresponds to the desired 0.5:2.5 ratio after correction and redox titration.

The co-precipitation step was carried out by adding 25 mL of 25% NH_4OH (Merck, India) solution dropwise (1 mL/min) into the mixed Fe–Co chloride solution under continuous stirring at 700 rpm, while maintaining the reaction temperature at 70 °C. The addition of NH_4OH was controlled to keep the pH in the range of 10–11, at which the mixed metal hydroxides and oxyhydroxides of Fe and Co readily form. After reaching the target pH, the suspension was aged under stirring for an additional 60 min to allow complete precipitation and growth of the nuclei. The resulting dense black precipitate, corresponding to the $Fe_{2.5}Co_{0.5}O_4$ precursor, was separated by filtration and washed repeatedly with distilled water until the filtrate reached approximately neutral pH to remove residual chloride and ammonium ions. The washed precipitate was then dried in an oven at 100°C for 1 h to remove residual moisture and lightly ground in an agate mortar to obtain a fine powder.

Band Gap Energy Calculation

Optical characterization was performed using a UV–Vis spectrophotometer (LW Scientific V-200-RS, USA) in the wavelength range of 200–800 nm to obtain the transmittance spectrum. The transmittance data were then transformed into absorbance using the equation [18]:

$$Absorbance\ (A) = 2 - \log_{10}(\%T) \tag{1}$$

The absorbance results are then used to calculate the band gap energy value using three optical approaches, namely:

1. Tauc Method (Direct and Indirect Band Gap)

This method is used to estimate the direct and indirect band gap energy values of semiconductor materials. The Tauc equation is expressed as [8]:

$$(\alpha h\nu)^n = A(h\nu - E_g) \tag{2}$$

In the Tauc equation, the coefficient α is the light absorption coefficient obtained from the transformation of the absorbance value to the optical path thickness (path length). The $h\nu$ value represents the photon energy, which is the product of Planck's constant (h) and the frequency of light (ν), which indicates the energy of the light used to stimulate the electronic transition. The A parameter is a material constant that depends on the type of transition and the electronic properties of the material being tested. Meanwhile, E_g is the band gap energy, which is the minimum energy required to move an electron from the valence band to the conduction band. The exponent value n indicates the type of optical transition that occurs: $n = 2$ is used for indirect allowed transitions, while $n = 1/2$ is used for direct allowed transitions. The Eg value is obtained by extrapolating a straight line on the graph $(\alpha h\nu)^n$ against hν, and finding the intersection point with the energy axis (X-axis) [8].

2. Kubelka-Munk Method (Diffuse Reflectance)

This method is used as an alternative approach for opaque solids or powders. The Kubelka-Munk function is defined as [20]:

$$F(R) = \frac{(1-R)^2}{2R} \tag{3}$$

where R is the diffuse reflectance. This function replaces α in the Tauc graph, so that the equation becomes:

$$[F(R) \cdot h\nu]^n = A(h\nu - Eg) \tag{4}$$

This method is more sensitive to surface conditions and is used to confirm the results of the Tauc method.

3. Urbach Energy Method (Eu)

To calculate the Urbach energy—which is related to the level of local irregularity or defects in the energy bands—the equation is used [21]:

$$\alpha = \alpha_0 \cdot exp\left(\frac{h\nu}{Eu}\right) \tag{5}$$

which after being converted into linear form produces:

$$ln(\alpha) = ln(\alpha_0) + \frac{h\nu}{Eu} \quad (6)$$

The Eu value is obtained from the inverse gradient of the straight line on the graph of $ln(\alpha)$ against hν. This value reflects the level of tail states due to dislocations, defects, or irregularities in the crystal structure [22].

RESULTS AND DISCUSSION

Tests were conducted using a UV–Vis spectrophotometer to obtain transmittance and absorbance curves of $Fe_{2.5}Co_{0.5}O_4$ nanoparticles in the wavelength range of 200–800 nm. These data were analyzed to determine the light absorption characteristics and used in the calculation of band gap energy and Urbach energy, the results of which are shown in Figure 1.

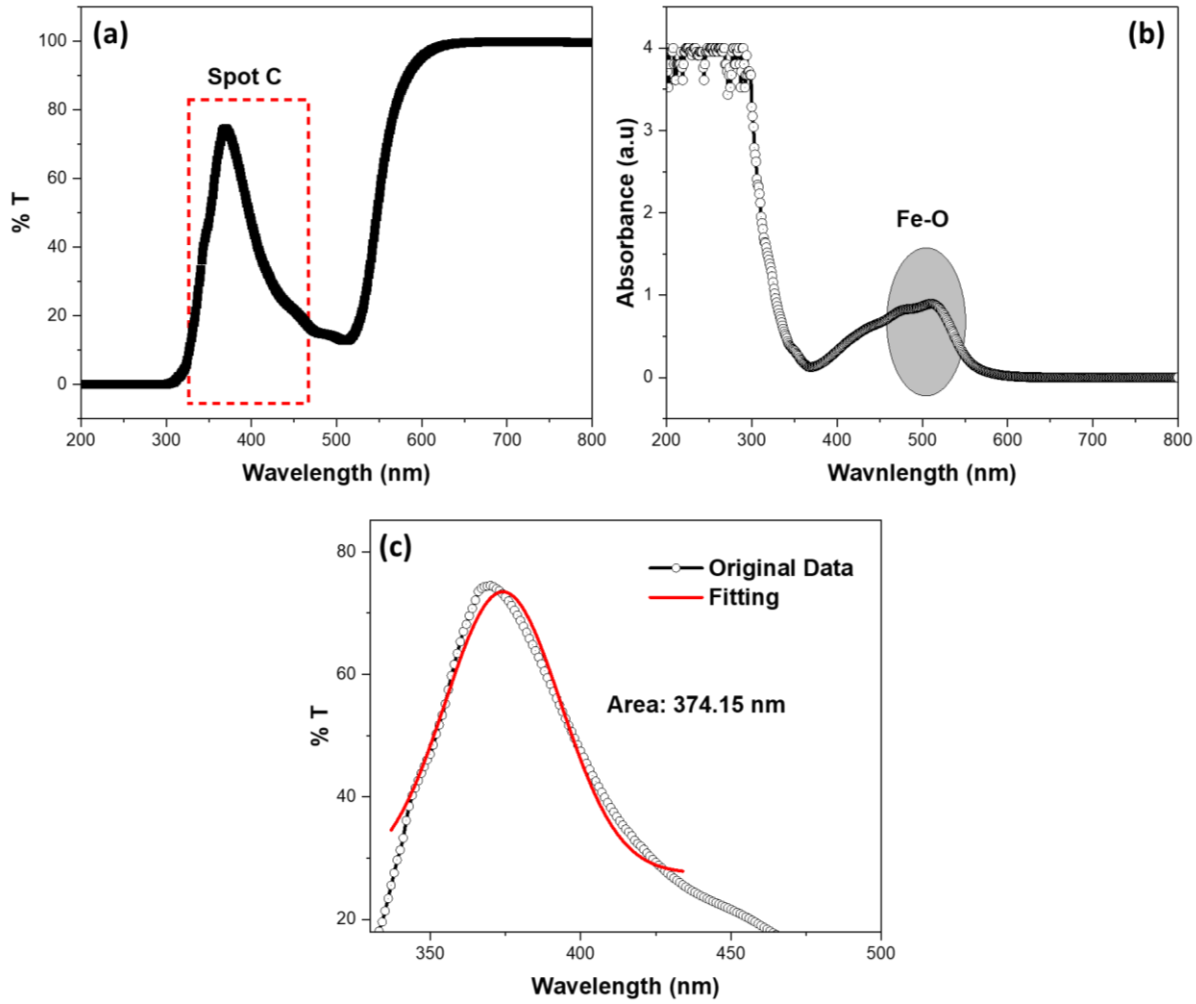

Figure 1. Graph of Absorbance Value of Cobalt-doped Magnetite

Figure 1 presents the transmittance (%T) curve as a function of wavelength for cobalt-doped magnetite nanoparticles, measured using a UV–Vis spectrophotometer in the range of 200–800 nm. The curve shows that the light transmittance reaches a minimum below 300 nm, indicating strong absorption by the material in the ultraviolet region. This behavior is commonly observed in materials with strong valence-to-conduction band transitions, particularly those involving Fe–O interactions within the spinel magnetite structure. In the wavelength range of 300–500 nm, marked as Spot C, significant fluctuations were observed, with the transmittance reaching a maximum of over 70% around 360–370 nm, followed by a sharp decrease to approximately 20% above 450 nm. This pattern suggests the presence of specific optical transition phenomena influenced by the incorporation of Co^{2+} ions as a result of doping. The shift and emergence of transmittance peaks in the visible region

(Spot C) indicate that cobalt doping modifies the electronic band structure, introducing new localized energy states that enable additional electronic transitions.

This phenomenon can be scientifically explained by considering that Co^{2+} ions substituting a fraction of Fe^{2+} ions at octahedral sites can modify the Co–O–Fe superexchange interaction. Such substitution alters not only the electronic structure but also increases band separation, which gives rise to additional optical absorption and affects the optical transparency window. Comparisons with previous studies support these findings. González-Sánchez et al. [23] reported that in cobalt ferrite nanoparticles, the main absorption peak occurs below 400 nm, and increasing cobalt doping induces a shift of the absorption edge toward shorter wavelengths (blue shift), leading to a widened band gap. Moreover, Zheng et al. [24] also reported the presence of dual optical transitions in transition-metal-doped ferrites, consisting of peaks in both the UV and visible regions, which were attributed to combined effects of metal–oxygen transitions and surface structural defects.

Figure 1(c) (inset) displays the fitted transmittance curve in the 340–480 nm wavelength region, showing a maximum peak at 374.15 nm. This peak corresponds to the wavelength at which the highest transmittance was recorded, serving as a crucial indicator for evaluating specific optical transitions within the material. The presence of a peak at 374.15 nm suggests that the material exhibits relatively high transparency to light at this wavelength, before decreasing again due to enhanced absorption. Scientifically, this indicates the occurrence of strong electronic transitions near 374 nm, which can be associated with transitions from intermediate energy states formed by the incorporation of Co^{2+} ions into the magnetite structure. These transitions are presumed to originate from the modification of the energy bands between the valence band (O 2p) and the conduction band (Fe 3d), where the presence of Co^{2+} creates new energy states or expands the existing band separation. This results in increased absorption selectivity in certain spectral regions, which is clearly reflected in the observed transmittance behavior. When compared with earlier studies, these findings are consistent with the work of Navalón et al. [25], who reported a characteristic absorption peak around 370–380 nm in Co^{2+} doped ferrites, attributing it to ligand-to-metal charge transfer (LMCT) between oxygen groups and transition metal ions. Similarly, Makuła et al. [26] noted that increasing cobalt doping in magnetite can tune the band structure, resulting in the appearance of new absorption peaks in the UV-visible region.

Figure 1(b) shows the absorbance curve (Absorbance vs. Wavelength) obtained by transforming the transmittance data. The spectrum reveals the optical absorption profile of cobalt-doped magnetite nanoparticles, with the highest absorbance occurring below 300 nm and a characteristic absorption peak around 500 nm, annotated as Fe–O. This curve provides important insights into the optical response of the material across the ultraviolet to visible range. In this transformation, the transmittance peak previously observed at 374 nm (high transmittance) appears as an absorbance trough, while the low-transmittance region near 500 nm now appears as a strong absorbance peak, indicating an area of intense photon energy absorption. The absorbance peak at 500 nm suggests that after cobalt doping at x = 0.5, the absorption position of the Fe–O transition shifts to slightly higher wavelengths compared to pure magnetite, which typically shows absorption below 470 nm. This implies that cobalt doping induces a shift in the Fe–O absorption peak toward longer wavelengths, reflecting local electronic structure modification while still maintaining good structural order.

The location of this absorption peak is particularly significant, as it forms the basis for subsequent band gap energy analysis. The peak at 500 nm also reflects the specific interactions of metal cations in octahedral coordination, particularly within the mixed spinel structure of $Fe_{2.5}Co_{0.5}O_4$, where a fraction of Fe^{2+}/Fe^{3+} ions are replaced by Co^{2+}. Du et al. [27] similarly reported that absorption peaks in cobalt-doped ferrites typically appear in the range of 480–530 nm, which are associated with d–d transitions and complex charge-transfer processes.

Subsequently, the E_g analysis was performed using four different approaches: direct and indirect band gap methods, the Kubelka–Munk function, and Urbach energy calculations, as summarized in Figure 2. In the Tauc-based evaluation, the absorption coefficient α and photon energy $h\nu$ were obtained from the UV–Vis absorbance data and used to construct $(\alpha h\nu)^n$ versus $h\nu$ plots as described in the corresponding Tauc relations (Equation 1 and Equation 2). For the Kubelka–Munk approach, the diffuse reflectance R was converted into the Kubelka–Munk function F(R) from the

transmittance data, expressed in terms of the molar absorption coefficient K and scattering factor S according to Equation 3, and the band gap was extracted from $[F(R)hv]^n$ versus hv plots following Equation. (4). The Urbach energy E_u was finally obtained by plotting $ln(\alpha)$ as a function of hνh\nuhν and determining the slope in the exponential tail region in accordance with Equation 5 and Equation 6.

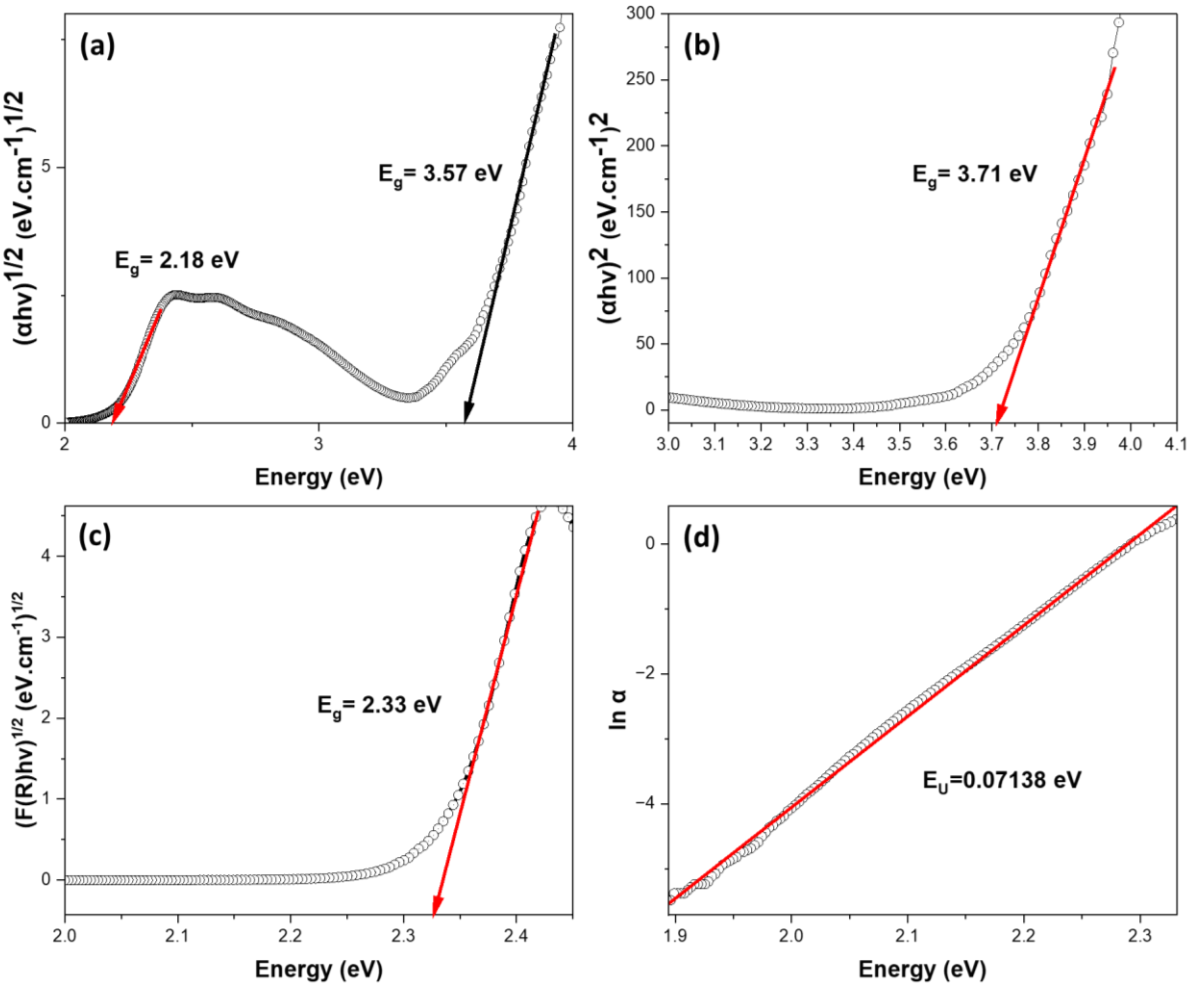

Figure 2. Calculation of Cobalt Doped Magnetite Nanoparticles (a) In-Direct Band Gap Energy of using Tauc Curve Method; (b) Direct band gap energy using Tauc Curve Method; (b) In-Direct band gap energy using Kubelka-Munk Method; (c) Urbach Energy

Figure 2(a) presents the calculation results of the indirect band gap energy of $Fe_{2.5}Co_{0.5}O_4$ nanoparticles using the Tauc method. The plot shows two linear fits with intercepts at 2.18 eV and 3.57 eV, respectively, indicating the presence of two distinct optical transitions. This phenomenon suggests that the investigated material does not exhibit a single dominant optical transition, but rather two indirect transition pathways that can occur simultaneously within the electronic structure. The value of 2.18 eV likely corresponds to energy transitions originating from regions with structural distortions or crystalline defects induced by cobalt doping. Such defects may include oxygen vacancies or disruptions in lattice periodicity due to the substitution of Fe^{3+} sites with Co^{2+} ions, which create localized energy levels within the main band gap [28]. These localized levels enable electrons to undergo optical transitions from the valence band to the localized states before reaching the conduction band, thereby producing a lower band gap value.

Meanwhile, the 3.57 eV value can be associated with the primary transition from more homogeneous crystalline regions, where electron–hole interactions occur under ideal conditions without significant defects. This indicates that cobalt doping does not entirely degrade the structure but can in fact broaden the band gap energy through orbital interactions between Co and Fe 3d states within the spinel lattice [29]. Such interactions enhance conduction band rigidity and increase the

energy required for electron excitation. The coexistence of these two band gap values has also been reported in similar studies. Mishra et al. [29] observed that cobalt-substituted ferrite nanoparticles can display dual band gap values reflecting the presence of mixed phases or local variations in electronic structure. Similarly, Anantharamaiah and Joy [28] showed that $CoFe_2O_4$ systems, when controlled in size and dopant distribution, exhibit two modes of optical transitions arising from modifications in the density of states and the formation of forbidden levels within the main bands.

Figure 2(b) illustrates the direct band gap energy of cobalt-doped magnetite ($Fe_{2.5}Co_{0.5}O_4$), determined using the Tauc plot with $(\alpha h\nu)^2$ versus photon energy (hν). From the linear fitting performed on the steep absorption edge above 3.5 eV, the direct band gap value was calculated as 3.71 eV. This value is relatively higher compared to pure magnetite, which typically exhibits a direct band gap of around 2.0–2.2 eV. This increase can be explained by several mechanisms. First, the substitution of Fe^{3+} ions with Co^{2+} in the inverse spinel lattice may cause local distortions in the crystal structure and alter the electronic energy levels in the valence and conduction bands. Cobalt has a different electronic configuration and forms stronger bonds with oxygen compared to iron, which may drive the widening or shifting of the energy bands. Second, these changes may lead to an enhancement in direct optical transitions, as Co^{2+} doping also increases lattice order and strengthens metal–oxygen (M–O) bond regularity, thereby improving UV absorption and enlarging the band gap. This finding is consistent with the study by Monfared et al. [30], who reported that transition-metal substitution in ferrite nanosystems can increase the direct band gap to above 3.5 eV depending on dopant type and concentration. Furthermore, the preferential occupation of octahedral sites by Co^{2+} can result in larger crystal field splitting, thereby increasing band separation. This is in line with Makuła et al. [26], who reported that in Co-based ferrites, increasing dopant concentration enhances band gap energy due to greater overlap of metal–oxygen orbitals, leading to sharper and more efficient transitions.

In addition to the indirect band gap analysis using the Tauc method, Figure 2(c) shows the estimation of the indirect band gap energy of cobalt-doped magnetite nanoparticles ($Fe_{2.5}Co_{0.5}O_4$) using the Kubelka–Munk function. The obtained indirect band gap was 2.33 eV, slightly higher than the Tauc method result of 2.18 eV. Such discrepancies are common because the Kubelka–Munk approach is based on diffuse reflectance data and is more sensitive to surface morphology and particle characteristics in powdered or opaque samples [16]. In contrast, the Tauc method derived from absorbance data better represents photon transitions in transparent materials or thin films. Thus, the 2.33 eV value obtained from Kubelka–Munk can be regarded as a validation that the indirect band gap lies in this range, even though different methods yield slightly varying values.

Furthermore, Figure 2(d) shows the calculated E_U of 0.07138 eV, which reflects the presence of tail states caused by structural defects or local lattice disorder. When compared with the previously obtained direct band gap of 3.71 eV (Figure 2b), the indirect band gap values of 2.18 eV (Tauc) and 2.33 eV (Kubelka–Munk), it can be concluded that this material exhibits two electronic transition pathways: direct and indirect. The large difference of more than 1.3 eV between the direct and indirect band gap values indicates that cobalt doping significantly modifies the band structure, widening the direct band gap while maintaining the presence of a lower-energy indirect gap. This duality contributes to the optical properties of the material, particularly for photocatalytic and sensing applications, where indirect transitions dominate the absorption of longer-wavelength (lower-energy) [16]. The relatively small Urbach energy value (<0.1 eV) further indicates that despite modifications induced by doping, the material disorder remains low. This is consistent with the sharp absorption edge observed in the spectra, as opposed to the broadened absorption typically seen in amorphous or highly disordered materials [24].

CONCLUSION

This study successfully synthesized cobalt-doped magnetite ($Fe_{2.5}Co_{0.5}O_4$) nanoparticles from natural iron sand using the coprecipitation method and demonstrated that cobalt doping significantly influences the optical properties of the material. UV-Vis spectroscopic characterization revealed that Co^{2+} doping altered the transmittance and absorbance patterns, marked by the emergence of new absorption peaks and a redshift toward longer wavelengths. The band gap energies calculated using

three approaches (Tauc direct, Tauc indirect, and Kubelka–Munk) confirmed the coexistence of two optical transition pathways, namely direct and indirect, with values of 3.71 eV (direct), 2.18 eV (indirect-Tauc), and 2.33 eV (indirect-Kubelka–Munk), respectively. Furthermore, the relatively low Urbach energy (0.07138 eV) indicated that the crystalline structure remained well-ordered despite modifications induced by doping. These findings are consistent with previous literature, which reported that transition-metal substitutions such as Co^{2+} can increase the band gap and create new localized energy states that affect the optical properties. Future work may be directed toward exploring different Co^{2+} doping concentrations to establish a quantitative relationship between doping level and changes in optical properties, and coupling such optical studies with photocatalytic performance tests (under visible-light irradiation) and detailed magnetic characterization to fully assess the potential of $Fe_{2.5}Co_{0.5}O_4$ nanoparticles for photocatalytic and optoelectronic applications.

ACKNOWLEDGEMENT

This research was conducted in the Laboratory of Materials Physics, so we would like to express our sincere appreciation to our team. Our gratitude is also extended to our students who helped carry out sample preparation and data collection. Universitas Mataram supported this research under Contract Number 2282/UN18.L1/PP/2025 PDP on behalf of Kormil Saputra. The author gratefully acknowledges this support.

REFERENCES

[1] J. Langer, J. Quist, and K. Blok, 'Review of Renewable Energy Potentials in Indonesia and Their Contribution to a 100% Renewable Electricity System', *Energies*, vol. 14, no. 21, Art. no. 21, Jan. 2021, doi: 10.3390/en14217033.

[2] A. Khosla, V. Chaudhary, and H. Zhang, 'A paradigm of microbe-mediated green nano-semiconductors and nano-metals', *Nanotechnology*, no. Query date: 2025-05-14 09:44:32, 2024, doi: 10.1088/1361-6528/ad9aaf.

[3] L. Liu, X. Yan, Y. Zhang, D. Deng, H. He, and ..., 'Mn3O4–CeO2 Hollow Nanospheres for Electrochemical Determination of Hydrogen Peroxide', *ACS Applied Nano* …, no. Query date: 2025-05-14 09:44:32, 2023, doi: 10.1021/acsanm.2c05123.

[4] K. Saputra, S. Sunaryono, S. Hidayat, H. Wisodo, and A. Taufiq, 'Investigation of nanostructural and magnetic properties of Mn0.25Fe2.75O4/AC nanoparticles', *Materials Today: Proceedings*, vol. 44, pp. 3350–3354, Jan. 2021, doi: 10.1016/j.matpr.2020.11.646.

[5] K. Saputra, S. Sunaryono, N. V. Difa, S. Hidayat, and A. Taufiq, 'The effect of Zn doping on thermal properties and antimicrobial of ZnxFe2-xO3 nanoparticles', *AIP Conference Proceedings*, vol. 2251, no. 1, p. 040040, Aug. 2020, doi: 10.1063/5.0015679.

[6] A. G. Leonel *et al.*, 'Tunable magnetothermal properties of cobalt-doped magnetite–carboxymethylcellulose ferrofluids: smart nanoplatforms for potential magnetic hyperthermia applications in cancer therapy', Feb. 2021, doi: 10.1039/D0NA00820F.

[7] H. Akbi *et al.*, 'Preventing Agglomeration and Enhancing the Energetic Performance of Fine Ammonium Perchlorate through Surface Modification with Hydrophobic Reduced Graphene Oxide', *ChemistrySelect*, vol. 9, no. 1, p. e202301795, 2024, doi: 10.1002/slct.202301795.

[8] J. Tauc, 'Optical Properties of Amorphous Semiconductors', in *Amorphous and Liquid Semiconductors*, J. Tauc, Ed., Boston, MA: Springer US, 1974, pp. 159–220. doi: 10.1007/978-1-4615-8705-7_4.

[9] N. Kadian, R. Kumari, A. Panchal, J. Dalal, and D. Padalia, 'Structural and optical properties of gadolinium doped-magnetite nano-crystal for photocatalytic application', *Journal of Alloys and Compounds*, vol. 960, p. 170811, Oct. 2023, doi: 10.1016/j.jallcom.2023.170811.

[10] I. D. Fajariman *et al.*, 'Comparative Behavior Of Magnetic Iron Oxide Nanoparticles (Mions) Via Mechanical And Chemical Routes', *Indonesian Physical Review*, vol. 8, no. 1, pp. 181–195, 2025, doi: 10.29303/ipr.v8i1.407.

[11] E. Garaio *et al.*, 'A wide-frequency range AC magnetometer to measure the specific absorption rate in nanoparticles for magnetic hyperthermia', *Journal of Magnetism and Magnetic Materials*, vol. 368, pp. 432–437, Nov. 2014, doi: 10.1016/j.jmmm.2013.11.021.

[12] S. Susilawati, A. Doyan, and S. Hadisaputra, 'Analysis Magnetic Mineral Content of Natural Iron Sand in Beach Island Lombok as Basic Materials of Micro Wave Absorbers', *Jurnal Penelitian Pendidikan IPA*, vol. 8, no. 4, pp. 1755–1758, Oct. 2022, doi: 10.29303/jppipa.v8i4.2274.

[13] A. Taufiq *et al.*, 'Effects of ZnO nanoparticles on the antifungal performance of Fe3O4/ZnO nanocomposites prepared from natural sand', *Adv. Nat. Sci: Nanosci. Nanotechnol.*, vol. 11, no. 4, p. 045004, Sept. 2020, doi: 10.1088/2043-6254/abb8c6.

[14] A. Taufiq *et al.*, 'Nanoscale Clustering and Magnetic Properties of MnxFe3−xO4 Particles Prepared from Natural Magnetite', *J Supercond Nov Magn*, vol. 28, no. 9, pp. 2855–2863, Sept. 2015, doi: 10.1007/s10948-015-3111-9.

[15] C. Karthikeyan *et al.*, 'Biocidal chitosan-magnesium oxide nanoparticles *via* a green precipitation process', *Journal of Hazardous Materials*, vol. 411, p. 124884, June 2021, doi: 10.1016/j.jhazmat.2020.124884.

[16] H. Todou Assaouka *et al.*, 'Copper and iron co-doping effects on the structure, optical energy band gap, and catalytic behaviour of Co 3 O 4 nanocrystals towards low-temperature total oxidation of toluene', *Energy Advances*, vol. 2, no. 6, pp. 829–842, 2023, doi: 10.1039/D3YA00082F.

[17] D. Lachowicz *et al.*, 'Enhanced hyperthermic properties of biocompatible zinc ferrite nanoparticles with a charged polysaccharide coating', *J. Mater. Chem. B*, vol. 7, no. 18, pp. 2962–2973, May 2019, doi: 10.1039/C9TB00029A.

[18] A. S. Masotti, Á. B. Onófrio, E. N. Conceição, and A. M. Spohr, 'Uv–vis spectrophotometric direct transmittance analysis of composite resins', *Dental Materials*, vol. 23, no. 6, pp. 724–730, June 2007, doi: 10.1016/j.dental.2006.06.020.

[19] B. M. Haque, D. B. Chandra, P. Jiban, I. Nurul, and Z. Abdullah, 'Influence of Fe2+/Fe3+ ions in tuning the optical band gap of SnO2 nanoparticles synthesized by TSP method: Surface morphology, structural and optical studies', *Materials Science in Semiconductor Processing*, vol. 89, pp. 223–233, Jan. 2019, doi: 10.1016/j.mssp.2018.09.023.

[20] L. Yang and B. Kruse, 'Revised Kubelka–Munk theory. I. Theory and application', *J. Opt. Soc. Am. A, JOSAA*, vol. 21, no. 10, pp. 1933–1941, Oct. 2004, doi: 10.1364/JOSAA.21.001933.

[21] S. Benramache, Y. Aoun, S. Lakel, B. Benhaoua, and C. Torchi, 'The calculate of optical gap energy and urbach energy of Ni1−xCoxO thin films', *Sādhanā*, vol. 44, no. 1, p. 26, Jan. 2019, doi: 10.1007/s12046-018-1003-y.

[22] M. Ledinsky *et al.*, 'Temperature Dependence of the Urbach Energy in Lead Iodide Perovskites', *J. Phys. Chem. Lett.*, vol. 10, no. 6, pp. 1368–1373, Mar. 2019, doi: 10.1021/acs.jpclett.9b00138.

[23] M. González-Sánchez, H. Khadhraoui, and ..., 'Non-enzymatic glucose sensor using mesoporous carbon screen-printed electrodes modified with cobalt phthalocyanine by phase inversion', *Microchemical …*, no. Query date: 2025-05-14 09:44:32, 2024, [Online]. Available: https://www.sciencedirect.com/science/article/pii/S0026265X24004260

[24] Y. Zheng, R. Gao, Y. Qiu, L. Zheng, Z. Hu, and X. Liu, 'Tuning Co2+ Coordination in Cobalt Layered Double Hydroxide Nanosheets via Fe3+ Doping for Efficient Oxygen Evolution', *Inorg. Chem.*, vol. 60, no. 7, pp. 5252–5263, Apr. 2021, doi: 10.1021/acs.inorgchem.1c00248.

[25] S. Navalón, A. Dhakshinamoorthy, M. Álvaro, B. Ferrer, and H. García, 'Metal–Organic Frameworks as Photocatalysts for Solar-Driven Overall Water Splitting', *Chem. Rev.*, vol. 123, no. 1, pp. 445–490, Jan. 2023, doi: 10.1021/acs.chemrev.2c00460.

[26] P. Makuła, M. Pacia, and W. Macyk, 'How To Correctly Determine the Band Gap Energy of Modified Semiconductor Photocatalysts Based on UV–Vis Spectra', *J. Phys. Chem. Lett.*, vol. 9, no. 23, pp. 6814–6817, Dec. 2018, doi: 10.1021/acs.jpclett.8b02892.

[27] C. Du *et al.*, 'In situ synthesis of oxygen-doped carbon quantum dots embedded in MIL-53(Fe) for efficient degradation of oxytetracycline', *Environ Sci Pollut Res*, vol. 31, no. 18, pp. 26686–26698, Apr. 2024, doi: 10.1007/s11356-024-32729-9.

[28] P. N. Anantharamaiah and P. A. Joy, 'Effect of co-substitution of Co2+ and V5+ for Fe3+ on the magnetic properties of CoFe2O4', *Physica B: Condensed Matter*, vol. 554, pp. 107–113, Feb. 2019, doi: 10.1016/j.physb.2018.11.031.

[29] D. Mishra, J. Nanda, S. Parida, K. J. Sankaran, and S. Ghadei, 'Effect of Y3+ and Co2+ co-doping on the structural, optical, magnetic and dielectric properties of LaFeO3 nanoparticles', *J Sol-Gel Sci Technol*, vol. 111, no. 2, pp. 381–394, Aug. 2024, doi: 10.1007/s10971-024-06452-3.

[30] A. H. Monfared, A. Zamanian, I. Sharifi, and M. Mozafari, 'Reversible multistimuli-responsive manganese–zinc ferrite/P(NIPAAM-AAc-AAm) core-shell nanoparticles: A programmed ferrogel system', *Materials Chemistry and Physics*, vol. 226, pp. 44–50, Mar. 2019, doi: 10.1016/j.matchemphys.2019.01.016.